ISSN 0021-3640, JETP Letters, 2010, Vol. 91, No. 8, pp. 382–386. © Pleiades Publishing, Inc., 2010.
Original Russian Text © V.V. Moskalenko, I.V. Soboleva, A.A. Fedyanin, 2010, published in Pis'ma v Zhurnal Éksperimental'noĭ i Teoreticheskoĭ Fiziki, 2010, Vol. 91, No. 8, pp. 414–418.

Surface Wave-Induced Enhancement of the Goos–Hänchen Effect in One-Dimensional Photonic Crystals¶

V. V. Moskalenko[a], I. V. Soboleva[a, b], and A. A. Fedyanin[a]

[a] *Moscow State University, Moscow, 119991 Russia*
e-mail: fedyanin@nanolab.phys.msu.ru
[b] *Frumkin Institute of Physical Chemistry and Electrochemistry, Moscow, 119991 Russia*

Received March 16, 2010

The excitation conditions of surface electromagnetic waves in one-dimensional photonic crystals (Bragg reflectors) are studied. Surface electromagnetic waves are visualized by the far-field optical microscopy of the surface of the photonic crystal. The enhancement of the Goos–Hänchen effect by surface electromagnetic waves excited in one-dimensional photonic crystals has been experimentally observed. The Goos–Hänchen shift reaches 30λ for a wavelength of $\lambda = 532$ nm.

DOI: 10.1134/S0021364010080047

The Goos–Hänchen effect is the lateral shift of a totally reflected beam relative to a beam reflected from a perfect mirror (Fig. 1). The effect was observed for the first time in 1943 by Goos and Hänchen for multiple reflections in a glass plate [1]; the shift detected was as large as $1-2\lambda$ for a wavelength of 578 nm. There are several approaches to explain the Goos–Hänchen effect. The first one, the so-called phase method [2, 3], is based on the phase shift between the incident and reflected beams appearing during total internal reflection (TIR). If the linearly polarized beam is considered as a wave packet limited in space, the shift D of the reflected beam is determined from the Fresnel equations as

$$D = -\frac{\lambda}{2\pi}\frac{\partial\varphi(\theta)}{\partial\theta}, \quad (1)$$

where λ is the wavelength, $\varphi(\theta)$ is the phase of the complex reflection coefficient, and θ is the angle of incidence. If the polarization of the incident beam differs from the linear one, the polarization dependence of the phase $\varphi(\theta)$ leads to two independent linearly polarized components shifted at different distances.

Another way to explain the Goos–Hänchen effect is suggested in [4]. In the TIR case, there is an evanescent field on the dielectric surface. The energy flux through the surface perpendicular to the incident plane and to the interface is nonzero, and the intensities of the incident and reflected beams are equal. Thus, the energy conservation law is fulfilled if the reflected beam shift appears.

The Goos–Hänchen effect can be significantly enhanced in absorbing media [5–7] or in the case of an additional energy flux at the interface caused by the propagation of a surface electromagnetic wave (SEW) [8, 9]. Surface plasmon polaritons (SPP) are an example of such SEWs. In [8], the Goos–Hänchen shift was measured for the beam reflected from the metallic diffraction grating near the Wood anomaly for the resonant SPP excitation. The maximal shift value was 30λ for the incident wavelength of 3.39 μm. In [9], the surface plasmon was excited by using the Kretschmann configuration. The beam was observed to be shifted by more than 50λ for the wavelength of 632 nm, which corresponds to an enhancement of the Goos–Hänchen effect by more than 10 times relative to the shift in the case of total internal reflection from a dielectric surface.

The high sensitivity of the Goos–Hänchen shift value to the SPP characteristics allow for the use of this effect in optical sensors. An SPP sensor is based on the dependence of the SPP wave vector on the refraction index of the dielectric at the metal–dielectric interface. It causes high sensor sensitivity to the resonant conditions of the SPP excitation and the influ-

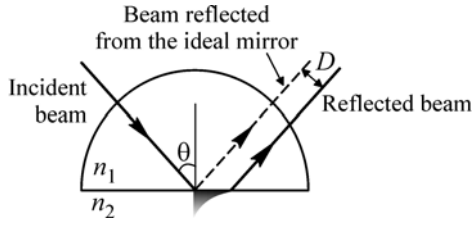

Fig. 1. Illustration of the Goos–Hänchen effect. The lateral shift D of the totally reflected beam ($n_1 > n_2$) is observed.

¶The article was translated by the authors.

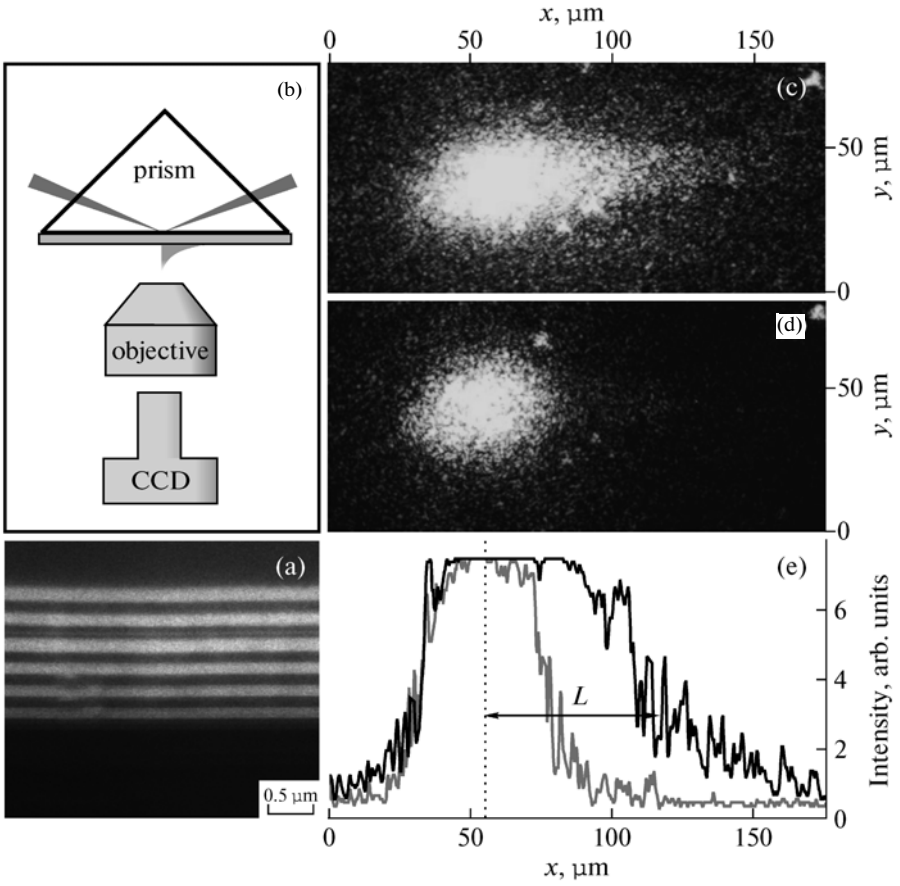

Fig. 2. (a) Scanning electron microscope image of the edge of the photonic crystal. (b) Sketch of the setup for the observation of the excitation of surface electromagnetic waves on the surface of the photonic crystal by using the optical microscopy technique. (c, d) Microimages of the surface of the photonic crystal for the incidence of *s*- and *p*-polarized light, respectively. (e) The intensity distribution along the centers of the spots for both polarizations of incident light.

ences of the dielectric environment on the SPP length and Goos–Hänchen shift value. The dependence of the Goos–Hänchen shift on the reflection coefficient of the dielectric medium under SPP excitation in the attenuated total reflection scheme was explored in [10]. The sensitivity of the sensor is 1.82×10^{-8} RIU/nm. The minimal Goos–Hänchen shift appeared to be 20 nm. This corresponds to a resolution of approximately 10^{-8} RIU, which is an order of magnitude better than for the other types of SPP sensors.

Surface electromagnetic waves can be excited on the surfaces of photonic crystals. There are wave equation solutions at photonic band gap frequencies corresponding to the SEWs [11, 12]. The dispersion curve of the incident light in a vacuum does not intersect with the SEW dispersion law, and the SEW excitation from a vacuum is impossible. The methods of attenuated total internal reflectance give the possibility of decreasing the slope of the light dispersion curve down to the SEW curve crossing. The experimental detection of the SEW on the surface of the photonic crystal was made in [11].

SEWs in photonic crystals are similar to surface plasmons by many optical properties but have some peculiarities [12]. First, the polarization conditions of SEW excitation are inverted relative to plasmons, and SEWs are excited solely for the *s*-polarized incident light. Second, the changing of the photonic crystal period provides a way to tune the SEW wavelength in the wide spectral range. Third, the SEW mean free path is significantly (4–5 times) larger than the plasmon one due to the low absorption in the dielectric layers. In [13], the Goos–Hänchen effect was theoretically considered in two-dimensional photonic waveguides. Due to the excitation of guided modes, the Goos–Hänchen effect was shown to be enhanced by more than one order of magnitude in comparison with the single TIR from the dielectric surface. At present, the experimental observation of the Goos–Hänchen effect in photonic crystals is absent.

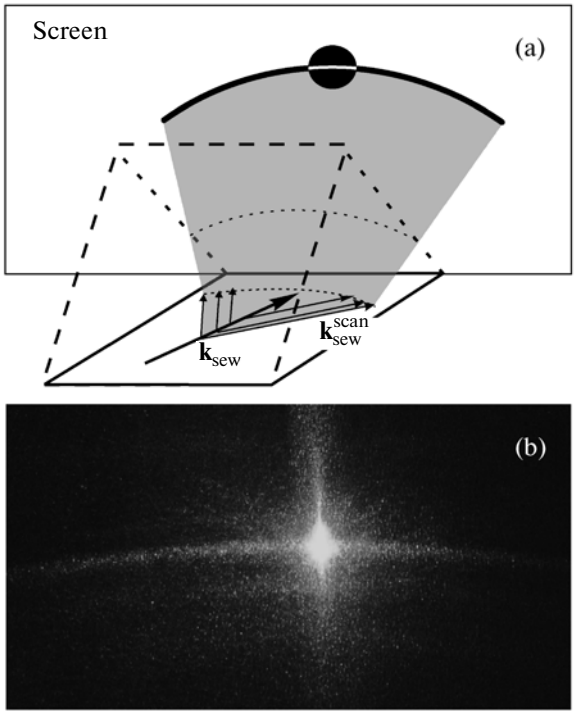

Fig. 3. (a) Schematic describing the scattering of surface electromagnetic waves in the plane of the propagation on the surface of the photonic crystal in the Kretschmann configuration; $\mathbf{k}_{sew}$ is the wave vector of the surface electromagnetic wave, and $\mathbf{k}_{sew}^{scatt}$ is the wave vector of the scattered component of the surface electromagnetic wave. (b) Scattering pattern of surface electromagnetic waves in the total reflection direction.

In this paper, the enhancement of the Goos–Hänchen effect due to SEW excitation in photonic crystals is observed and systematically studied.

Samples of 1D photonic crystals (Bragg reflectors) were fabricated using thermal thin-film deposition on a glass substrate and consisted of six bilayers of SiO_2/ZrO_2 with refractive indices of 1.46 and 1.9, respectively. The period of the photonic crystal has been determined by scanning electronic microscopy (Fig. 2a) and appeared to be 250 ± 10 nm. The multilayer was designed to exhibit SEWs on the outer surface of the photonic crystal with incident *s*-polarized light at an angle of incidence of 50°. The excitation and detection of the SEW were performed in a Kretschmann attenuated total reflection device (Fig. 2b). A glass substrate was connected to the prism using an index-matching liquid (aqueous solution of glycerol). The light source was a CW single-mode laser operating at $\lambda = 532$ nm with a power $P = 10$ mW and angular divergence of 2.5 mrad. A laser beam was focused on the surface of the photonic crystal by a collecting lens with a focal length of 25.4 mm on a spot with a diameter of 50 μm. The polarization of the light was controlled by a double Fresnel rhombus and a Glan prism. The angle of incidence on the inner surface of the photonic crystal was fixed at 50°. Visualization was performed by using the light scattered in the far field by optical microscopy [12] using an objective lens with a numerical aperture NA = 0.28 focused on the surface of the photonic crystal where the SEW was excited. The image was recorded by a CCD camera.

Figures 2c and 2d show the images of the surfaces of the photonic crystal upon the incident *s*- and *p*-polarized light. For the *s*-polarized (Fig. 2c) incident light, the conditions of the SEW resonance are satisfied and the SEW is spatially distributed in a cometlike pattern strongly elongated in the propagation direction. The SEW mean free path can be estimated by using the "comet tail" length. In the case of *p*-polarized illumination (Fig. 2d), the image shows a pattern typical for TIR with a bright spot being a cross section of the beam reflected from the sample. Figure 2e shows the intensity profile along the centers of the spots for both cases. The profile shows the enlargement of the falling edge of the distribution at the SEW resonance. The SEW length is determined as the distance between the center of the *p*-polarized reflected spot and the level where the intensity decreases by $1/e$ times for the *s*-polarized beam. The SEW length is estimated to be approximately 70 μm for the studied sample.

The visualization of evanescent fields is impossible in ideal conditions, because the SEW is an evanescent wave and exponentially decays along the surface normal. Despite the fact that the dielectric layers of the photonic crystal have low absorption, the observed SEW length is finite. Therefore, there are alternative mechanisms of losses, one of them is associated with SEW scattering from surface roughnesses. As the SEW is excited, the rescattering goes in the plane and out of the surface plane of the photonic crystal. The part of the incident radiation rescattered out of the plane is detected by the microscope objective. In addition, there is scattering in the plane of the surface, as is shown in Fig. 3a. Part of the SEW with the wave vector $\mathbf{k}_{sew}$ scatters, changes direction, and acquires the wave vector $\mathbf{k}_{sew}^{scatt}$. In this case, the angle of reflection is different from the original one. The scattering pattern is represented by the arc schematically shown in Fig. 3a. Figure 3b shows a photograph of the screen placed perpendicular to the reflected light. Reflected light, which does not transform into an SEW, is seen as a white spot. The bright arc arises due to SEW excitation and the subsequent rescattering.

The direct visualization of the Goos–Hänchen effect was performed using the SEW microscopy technique schematically shown in Fig. 4. As the SEW was excited, the reflected beam undergoes a lateral shift. An ethanol solution of Rhodamine 6G (10^{-5} M) was added to the index-matching liquid in a 100 : 1 ratio. Rhodamine 6G dye was used for the visualization of

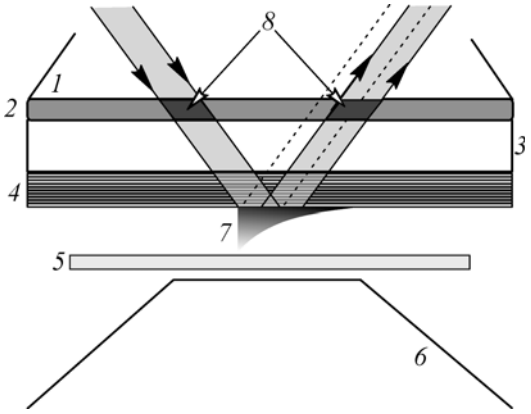

Fig. 4. Schematic of the visualization of the Goos–Hänchen effect: *1* is the prism, *2* is the index-matching fluid with the addition of an ethanol solution of Rhodamine 6G, *3* is the glass substrate coating 1D photonic crystal *4*, *5* are the OC13 orange filters, *6* is the objective, *7* is the surface electromagnetic wave, and *8* are the cross sections of the incident and reflected beams.

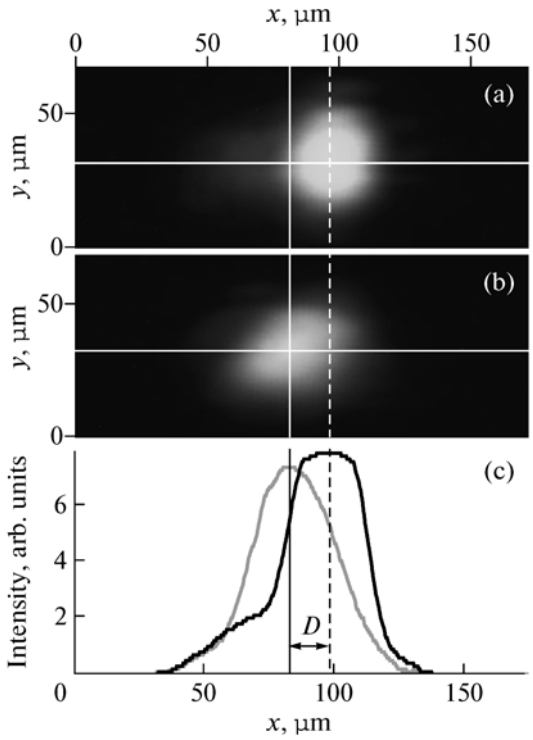

Fig. 5. Microimages of the fluorescence of the reflected beam in the cases of (a) the excitation of the surface electromagnetic wave by *s*-polarized light and (b) the absence of the surface electromagnetic wave in a *p*-polarized beam. (c) Fluorescence intensity profiles along the centers of the reflected beam cross sections, where the Goos–Hänchen shift is seen.

the incident and reflected beams. The OC13 orange filter was placed before the objective for the pump radiation cutoff and the observation of a sharp pattern of fluorescence. The Goos–Hänchen effect manifests itself in the shift of the cross section of the reflected spot for the *s*-polarized incident beam relative to the position of the reflected spot of the *p*-polarized beam.

Figures 5a and 5b show the cross sections of reflected *s*- and *p*-polarized beams (the spot of the incident beam is outside the frame). The intensity distributions of the fluorescence of the cross sections of reflected *s*- and *p*-polarized beams are shown in Fig. 5c. For the *p*-polarized light, the SEW is spatially distributed in the Gaussian profile with an intensity maximum corresponding to the center of the spot. As the reflected beam is *s*-polarized, the intensity maximum shifts toward the SEW propagation direction. This displacement achieving 16 μm is interpreted as the Goos–Hänchen shift.

For a single reflection configuration, the Goos–Hänchen shift reached the value of the wavelength [1, 14]. In the studied case, the shift value is approximately 30λ, thus, the enhancement of the Goos–Hänchen effect due to the additional lateral flux of energy in the SEW is more than one order of magnitude larger. The Goos–Hänchen shift in homogeneous absorbing media [8] can be comparable with the displacement obtained in a photonic crystal. However, the enhancement in the photonic crystal under proper conditions is expected to be even more significant. The optimal design of a 1D photonic crystal allows for the enhancement of the SEW lifetime and the efficiency of the energy transformation of the incident light. The calculations performed using optical transfer matrix technique demonstrate that the increase of the number of dielectric layers in the photonic crystal leads to the further enhancement of the length of the SEW associated with the Goos–Hänchen shift.

In conclusion, the SEW relaxation mechanisms are studied in one-dimensional photonic crystals (Bragg reflectors). The SEW scattering on the surface plane and to the far field is shown to be the main relaxation mechanism. The far-field scattering gives a way to visualize the SEW by the optical far-field microscopy of the surface of the photonic crystal. The Goos–Hänchen effect in the photonic crystals is detected. The Goos–Hänchen shift achieves 16 μm in a 1D photonic crystal with a thickness of 12 quarter-wavelength dielectric layers. The shift value shows the significant (more than one order of magnitude) enhancement of the Goos–Hänchen effect in photonic crystals relative to the dielectric surface.

The work was supported by the Russian Foundation for Basic Research and the Ministry of Education and Science of the Russian Federation (contract no. 02.740.11.0215).

REFERENCES

1. F. Goos and H. Hänchen, Ann. Phys. **436**, 333 (1947).

2. K. Artmann, Ann. Phys. **437**, 87 (1948).
3. K. W. Chiu and J. J. Quinn, Am. J. Phys. **40**, 1847 (1972).
4. R. H. Renard, J. Opt. Soc. Am. **54**, 1190 (1964).
5. W. J. Wild and C. L. Giles, Phys. Rev. A **25**, 2099 (1982).
6. M. Merano, A. Aiello, G. W. t'Hooft, et al., Opt. Express **15**, 15928 (2007).
7. P. T. Leung, C. W. Chen, and H.-P. Chiang, Opt. Commun. **276**, 206 (2007).
8. C. Bonnet, D. Chauvat, O. Emile, et al., Opt. Lett. **26**, 666 (2001).
9. X. Yin, L. Hesselink, Z. Liu, et al., Appl. Phys. Lett. **85**, 372 (2004).
10. X. Yin and L. Hesselink, Appl. Phys. Lett. **89**, 261108 (2006).
11. W. M. Robertson and M. S. May, Appl. Phys. Lett. **74**, 1800 (1999).
12. I. V. Soboleva, E. Descrovi, C. Summonte, et al., Appl. Phys. Lett. **94**, 231122 (2009).
13. T. Paul, C. Rockstuhl, C. Menzel, and F. Lederer, Phys. Rev. A **77**, 053802 (2008).
14. H. Gilles, S. Girard, and J. Hamel, Opt. Lett. **27**, 1421 (2002).